JTTEE5 4:245-251

Characterization of Microstructural Defects in Plasma-Sprayed Thermal Barrier Coatings

P. Bengtsson and T. Johannesson

Thermal barrier coatings with a NiCrAlY bond coating and a 1.5 mm thick zirconia top coating were air plasma sprayed onto a nickel-base substrate. The top coatings were deposited with the same spraying parameters except for the amount of external cooling, which varied from no cooling to the maximum available. This resulted in four sets of samples produced with different cooling conditions where substrate temperature varied from 100 to 830 °C. The coatings were examined by electron microscopy on polished surfaces and on fracture surfaces. The crack structure in the top coating was correlated to the substrate temperature. The density both of horizontal delaminations and of vertical microcracks was shown to decrease at higher substrate temperatures. The grain structure was columnar, and smaller grains were found at lower temperatures. Explanations for the differences in defect densities are discussed.

1. Introduction

THERMAL barrier coatings (TBCs) are frequently used as insulating materials on metallic parts in the hot section of jet engines. Such coatings can decrease the service temperature of the metallic material by about 100 °C or, equally important, can allow a higher combustion temperature in the engine to be chosen. The latter option is preferable because it leads to improved engine efficiency as well as lower emissions. Thus, many efforts are directed toward developing coatings with higher insulating properties.

The insulation effect can be increased by using new materials, by controlling microstructure, or by creating thicker coatings. Different types of coating defects, the effect of the spraying process (Ref 1), and modeling of possible defects in sprayed TBCs are discussed in the literature (Ref 2). Coating microstructure—including grain sizes, grain boundaries, and interfacial defects—also has been reviewed (Ref 3). These investigations have shown that the defect densities within the coatings vary with spraying parameters.

One particularly important process parameter in this regard is the substrate temperature during deposition.

In this study, 1.5 mm thick TBCs were produced by air plasma spraying at different substrate temperatures. The objective was to determine the influence of substrate temperature on the development of microstructure and defect structure, factors that determine TBC performance.

The study also identified the mechanisms that are active when the defects are created.

Keywords: defect density, microstructure, plasma spraying, substrate temperature, thermal barrier coating

P. Bengtsson, Volvo Aero Corporation, Trollhättan, Sweden (presently at Division of Engineering Materials, Department of Mechanical Engineering, Linköping University, S-581 83 Linköping, Sweden; **T. Johannesson,** Division of Materials Engineering, Department of Solid Mechanics, Lund University, S-221 00 Lund, Sweden

2. Experimental Procedures

2.1 *Materials*

The TBCs were sprayed onto a grit-blasted nickel-base substrate material, Hastelloy X. The chemical composition of the bond coating powder material was 67Ni-22Cr-10Al-1Y (wt%). Air plasma spraying was used to deposit both the bond coating and the top coating of ZrO_2 partially stabilized with 8 wt% Y_2O_3. The top coating feedstock had an agglomerated and sintered morphology.

2.2 *Deposition Process*

The bond coating and the top coating were deposited onto circular substrates, 25 mm in diameter and 6 mm thick. The spraying setup is shown in Fig. 1. The substrates were mounted on a cylindrical fixture that rotated with an angular velocity of 155 rev/min around its axle during deposition. Metco EG88 spraying equipment (Sulzer-Metco AB, Stockholm, Sweden) outfitted with a Metco 9MB plasma gun was used for the deposition process. The plasma gun moved vertically up and down the rotating specimens.

All substrates were first coated with a 100 μm thick bond coating. Before the top coating was sprayed, the bond-coated substrates were preheated to a temperature of 100 °C by moving the plasma gun without powder. Then, a 1500 μm thick zirconia top coating was sprayed onto the specimens.

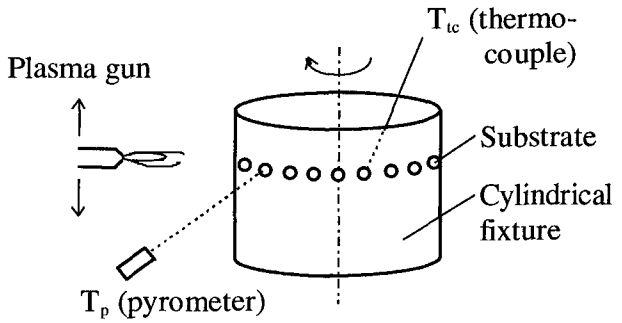

Fig. 1 Schematic of the experimental setup

Table 1 Cooling conditions for different samples

Cooling condition	Air jet pressure (front), bar	Pressurized air (front)	Liquid CO_2 (back)
1 (low cooling)	0	Off	Off
2 (intermediate)	1.2	Off	On
3 (intermediate)	2.4	Off	On
4 (high cooling)	4.8	On	On

Table 2 Measured steady-state temperatures for the samples

Cooling condition	Steady-state coating temperature (T_p^{ss}), °C	Steady-state substrate temperature (T_{tc}^{ss}), °C
1	830	830
2	640	640
3	410	500
4	325	355

Spraying parameters, except for substrate temperature, were held constant for all sprayed samples. Three different external cooling arrangements were used to produce coatings with different substrate temperatures during spraying. The first method employed air jets attached to and following the motion of the plasma gun. The pressure of the air jet was controlled and four different pressure levels selected. The second method used a stationary air jet that could be directed toward the surface of the specimens. Only "on" and "off" options were available. The third method used liquid CO_2 that could be sprayed onto the backs of the rotating samples from fixed nozzles.

Sets of samples were sprayed at four different cooling conditions (Table 1). Cooling condition 1 used no external cooling, and cooling condition 4 used all available methods to achieve maximum cooling. Conditions 2 and 3 were chosen to obtain temperature levels between the two extremes.

2.3 *Temperature Monitoring*

Temperature measurements were made with a pyrometer and a thermocouple during deposition. The pyrometer measured the surface temperature, T_p, of the growing coating at a point located 50 mm before the specimen entered the spray beam. This temperature will be referred to as the coating temperature. The thermocouples were placed in the substrates 0.5 mm below the interface with the bond coating. This allowed for continuous recording of the substrate temperature, T_{tc}.

The coating temperature during spraying showed a steep increase during the first passages of the plasma gun. When the coating thickness reached about 500 μm, a steady-state temperature (T^{ss}) occurred. The T_p fluctuated around this steady-state temperature as the plasma gun moved across the specimens.

2.4 *Microstructural Analysis*

Polished cross sections as well as fracture cross sections were prepared in order to examine the microstructure of the top coatings. The samples to be polished were first vacuum impregnated with epoxy and cured for 1 h at 75 °C. This allowed the epoxy to penetrate pores and cracks, preventing pullout of particles during polishing. The molded samples were then cut in the axial direction with a diamond saw and vacuum impregnated again. The resulting cross-sectional surface was polished using a Struers Prepamatic automatic polishing machine (Struers A/S, Copenhagen, Denmark). Cross-sectional fracture surfaces were obtained by first removing the substrate by diamond sawing and then breaking the coating system.

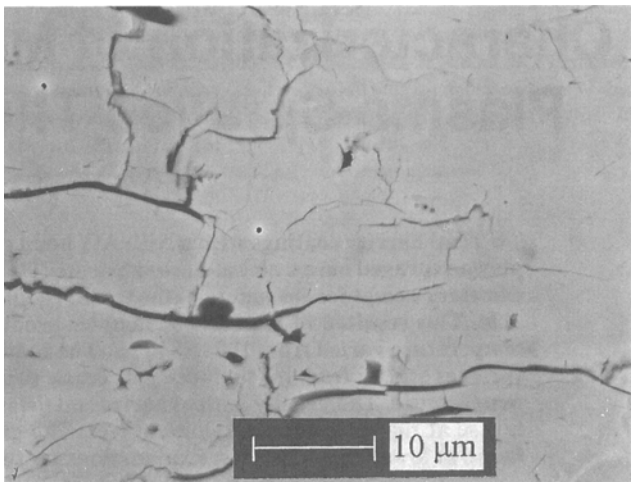

Fig. 2 Polished cross section revealing vertical microcracks and horizontal delaminations in a specimen sprayed at low cooling (cooling condition 1) where the steady-state temperature has been reached

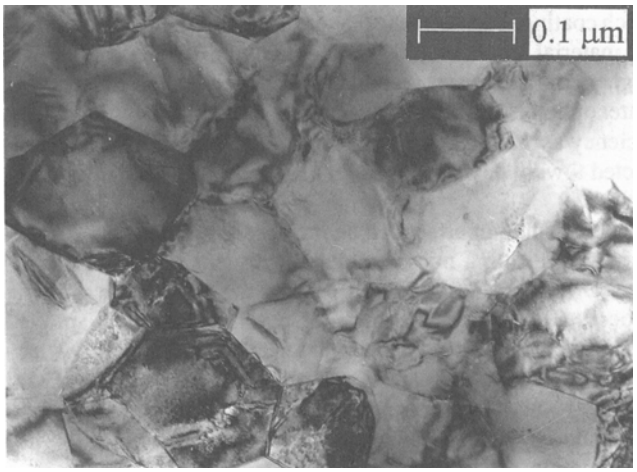

Fig. 3 Planar section where the steady-state temperature has been reached in a specimen sprayed at high cooling (cooling condition 4)

A scanning electron microscope (SEM) was used to determine the crack structures on polished cross sections. This analysis revealed a structure consisting of vertically oriented microcracks and horizontally oriented delaminations (Fig. 2). A vertical microcrack is defined as a crack having a length shorter than 20 μm and an orientation perpendicular to the interface between the top coating and the bond coating. A horizontal delamination is defined as any delamination, regardless of length, oriented parallel to the same interface. The densities of the defects were calculated using a point-counting technique by placing a grid with vertical and horizontal lines over the

Table 3 Densities of vertical microcracks and horizontal delaminations

Cooling condition	Density of vertical microcracks at 50 μm, mm^{-1}	Density of horizontal delaminations at 50 μm, mm^{-1}	Coating temperature when 50 μm is deposited, °C	Density of vertical microcracks at steady state, mm^{-1}	Density of horizontal delaminations at steady state, mm^{-1}	Steady-state coating temperature °C
1	84.4	97.6	305	38.8	48.4	830
2	79.3	96.4	295	43.7	60.7	640
3	75.8	90.6	250	66.9	104	410
4	80.7	111	210	72.2	102	325

Table 4 Top coating grain dimensions at steady-state conditions

Cooling condition	Grain width at steady state, μm	Grain height at steady state, μm
1	0.7	13
4	0.2	3

measurement area. The number of intersections between the horizontal delaminations and the vertical lines divided by the vertical line length gave the density (mm^{-1}) of horizontal delaminations. In the same way, the number of intersections between vertical microcracks and the horizontal lines gave the density (mm^{-1}) of vertical microcracks. The grid was placed at 16 different locations for each defect density measurement level within the top coating. The resulting standard deviation of the defect density values varied between 10 and 20 mm^{-1}.

Transmission electron microscopy (TEM) studies on both planar sections and cross-sectional samples of the top coating were performed from the upper region of the top coating, where the steady-state temperature was reached. The top coating was removed from the substrate by dissolving the bond coating in 50% HCl. Cylindrical samples, 3 mm in diameter, were cut from the top coating using an ultrasonic cutter and were polished to a thickness of 100 μm. The thickness was reduced further to about 20 μm by ball-dimpling each side of the surfaces with diamond paste. The final thinning of the samples to electron transparency was made by Ar^+ sputtering using a Gatan dual ion mill (Gatan Inc., Pleasanton, CA, USA).

3. Results

3.1 *Temperature Measurements*

Table 2 lists the recorded steady-state temperatures for the different cooling conditions. As shown, differences in cooling rate resulted in a variation of the substrate temperature from 355 to 830 °C.

3.2 *Defect Densities*

Polished cross sections were used to determine the crack and delamination densities in the samples. The first measurement point was situated 50 μm above the interface between the bond coating and the top coating, and a second point was in the upper part of the top coating, where the steady-state temperature was reached. Table 3 shows the densities of vertical microcracks and horizontal delaminations obtained in the coatings. The coating temperature recorded by the pyrometer when the coating had grown to the position of the first measurement point (50 μm) is included.

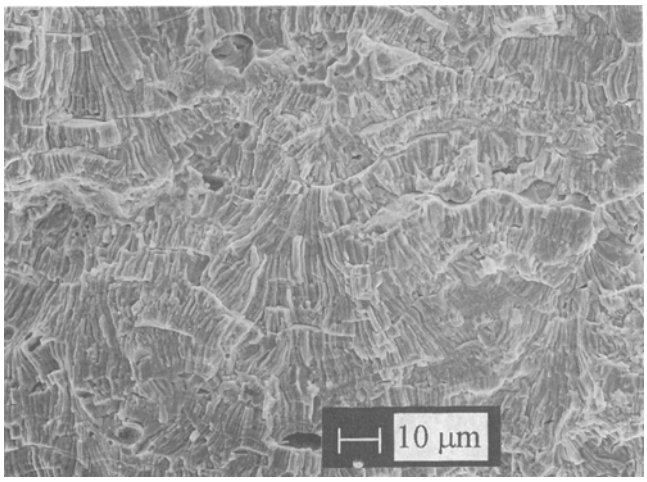

Fig. 4 Fracture surface where the steady-state temperature has been reached in a specimen sprayed at low cooling (cooling condition 1)

The size and geometry of the grains forming the coating were studied by SEM of the fracture surfaces, which revealed a columnar grain structure oriented perpendicular to the interface between the bond coating and the top coating. Transmission electron microscopy was used to determine the width of the grains in the upper part of the top coating, where a steady-state temperature prevailed. Figure 3 shows a TEM planar section of the sample sprayed at cooling condition 4; the grains are hexagonally shaped with a low dislocation density. The measured average grain sizes for the two extreme samples are given in Table 4, which shows that grain size decreases with increased cooling.

3.3 *Coating Growth*

The growth of the coating was studied through SEM examination of cross-sectional fracture surfaces. This method provides a good understanding of how the microstructure was created. Polished cross-sectional surfaces were used to quantify the features.

The microstructure from a region where the steady-state temperature has been reached in a specimen sprayed at low cooling (cooling condition 1) is shown in Fig. 4. The microstructure consists of lamellae that follow the geometry of the underlying material. Each lamella has a thickness of about 13 μm, which

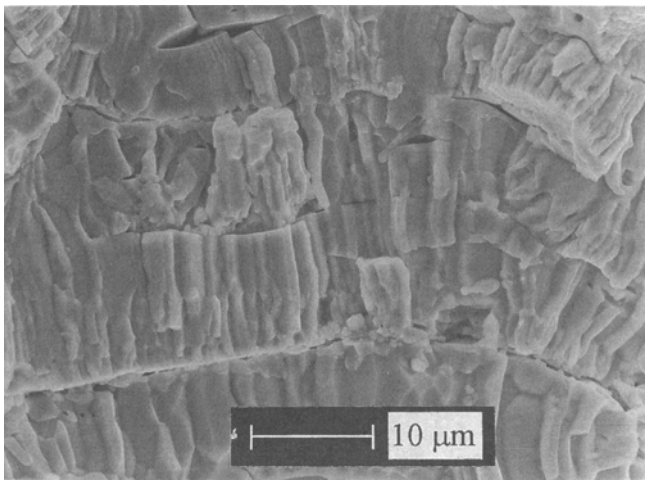

Fig. 5 High-magnification view of Fig. 4, revealing horizontal delaminations between lamellae

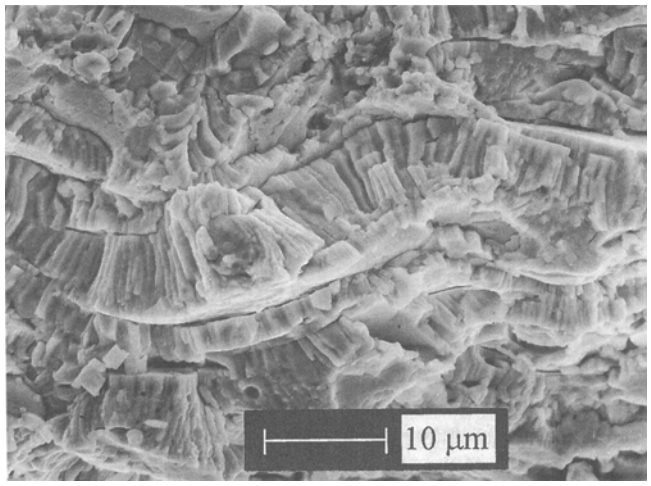

Fig. 6 Fracture surface where the steady-state temperature has been reached in a specimen sprayed at high cooling (cooling condition 4), revealing horizontal delaminations between both lamellae and splats

corresponds to the applied thickness from each passage of the plasma torch. Figure 5 shows the same structure at a higher magnification. No individual splats are visible within the lamellae; instead, the lamellae consist of columnar grains grown from the bottom to the top of the lamellae, perpendicular to the underlying material. Between the lamellae, horizontal delaminations are visible, indicating a zone with low cohesion.

Figure 6 shows the fracture surface from samples sprayed at high cooling (cooling condition 4) at the same magnification as for Fig. 5. In this case, a substructure of features resembling individual splats is observed within each lamellae. The splats are pancake-shaped with thicknesses of approximately 3 μm and diameters on the order of 100 μm. Inside the splats, vertically oriented columnar grains are found. The density of horizontal delaminations is much higher because delaminations occur between individual splats as well as between the lamellae. This makes it difficult to discriminate between the two different types of delaminations.

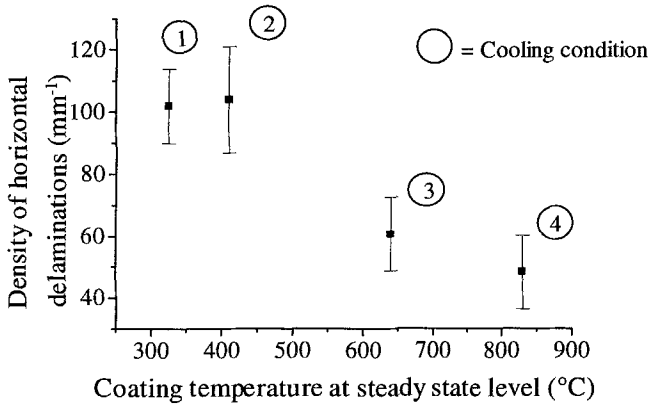

Fig. 7 Variation of density of horizontal delaminations with steady-state temperature

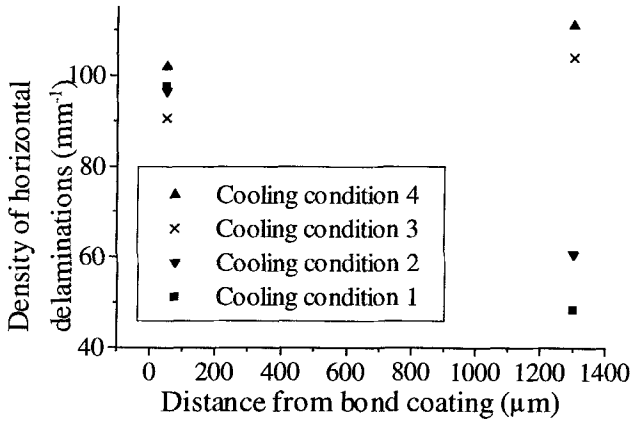

Fig. 8 Density of horizontal delaminations as a function of location in the ceramic coating

The measured densities of horizontal delaminations as a function of the steady-state temperature are shown in Fig. 7. High densities of horizontal delaminations are found at low steady-state coating temperatures (cooling conditions 3 and 4). Lower densities of horizontal delaminations are found at cooling conditions 1 and 2, where higher steady-state coating temperatures were reached. Close to the bond coating, all samples show structures with a high density of horizontal delaminations and the structure consists mainly of individual splats. This is understandable because the coating temperature at this location is almost the same for all cooling conditions. Figure 8 shows the density change of horizontal delaminations through the thickness of the coatings.

The density of vertical microcracks followed the same tendency. For all coatings, high densities of vertical microcracks were found close to the bond coating, where a low coating temperature was measured. When the steady-state coating temperature was reached, lower densities of vertical microcracks resulted—especially in cooling conditions 1 and 2, where higher steady-state temperatures were reached. In fact, the density of vertical microcracks is strongly correlated to the measured coating temperature during spraying (Fig. 9).

Based on the results obtained for the densities of horizontal delaminations and vertical microcracks, a schematic diagram

showing how the microstructure is built up during spraying is presented in Fig. 10. During deposition of the first lamella, the temperature will be comparatively low, independent of the cooling conditions. Therefore, large densities of horizontal delaminations and vertical microcracks will form. Samples sprayed with high external cooling will reach only a relatively low steady-state temperature, and, as for cooling condition 4, the only observed microstructural change with depth through the coating is a slight decrease in the density of vertical microcracks. More significant microstructural changes occur in samples sprayed without cooling. Samples from cooling condition 1, which reached a relatively high steady-state temperature, reveal a microstructure near the top with coarse grain size and low densities of both horizontal delaminations and vertical microcracks.

4. Discussion

The defects examined in this study are created when the molten droplets from the plasma flame impact on the underlying material and solidify. The injected ceramic powder is molten (with a temperature above the melting point) and is accelerated in the plasma flame. As soon as a droplet hits the underlying material, the droplet spreads out and heat is transported away. This involves not only heat conduction to the underlying material but also convection and radiation to the surrounding atmosphere. When the splat cools to the melting point, solidification commences heterogeneously at the interface between the splat and the underlying material (Ref 3). Grains nucleate and grow perpendicular to the surface of the underlying material, forming a columnar grain structure.

4.1 *Grain Size and Density of Horizontal Delaminations*

Samples sprayed at high cooling (cooling condition 4), where the steady-state temperature is low, show both a small grain diameter and a small grain height. Grain diameter is dependent on coating temperature: A low temperature results in high undercooling and a high nucleation rate. Hence, grains with small diameters are formed. The splat solidifies quickly due to the temperature gradient, and columnar grains grow throughout the thickness of the splat. As spraying continues, the same procedure is repeated for the droplets that follow. The interfaces between the splats are also boundaries between the grains and the cohesion is weak, thereby allowing a horizontal delamination. From the fracture surface of the coating it is clear that the density of horizontal delaminations is high under high cooling conditions, because individually solidified splats can be detected throughout the coating. Also, because the density of delaminations is constant throughout the coating, boundaries between the lamellae are difficult to detect after high cooling.

After the steady-state temperature has been reached under low cooling (cooling condition 1), a different microstructure is found. Larger grains, in both diameter and height, are present, and the density of horizontal delaminations is lower. As discussed before, the grain diameter is larger because the nucleation rate is lower due to the higher coating temperature. The grain height is larger compared to samples from cooling condi-

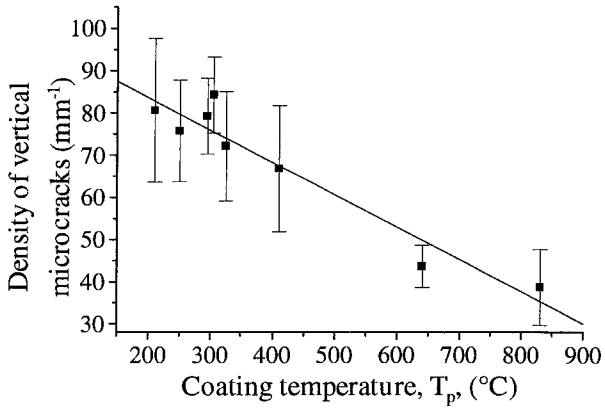

Fig. 9 Density of vertical microcracks as a function of coating temperature, measured both at steady state and close to the bond coating

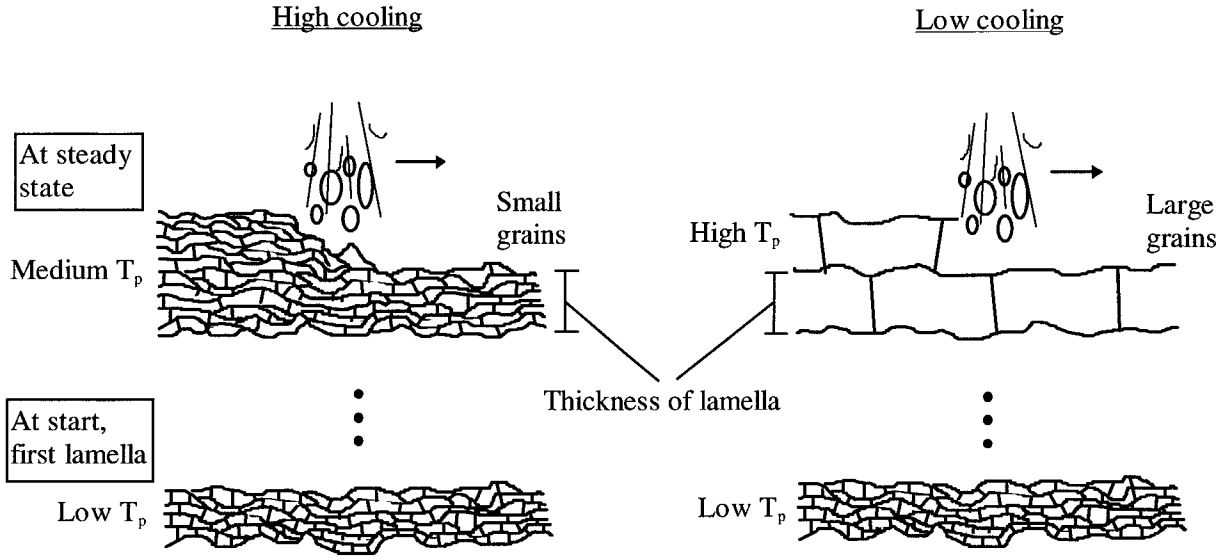

Fig. 10 General coating growth at different amounts of external cooling. Vertical microcracks and horizontal delaminations are shown.

tion 4 and equals the thickness applied in each passage (also referred to as "lamella") of the plasma gun. No individual splats are observed within these layers, and consequently there are no horizontal delaminations. The buildup of the layers is still made in the same way, with droplets impinging on newly solidified splats. In this case, however, the surface temperature is sufficiently high to allow continued grain growth through several splats. Thus, the grains traverse the splats with no discontinuity causing horizontal delaminations between the splats. This structure is found not only in the steady-state region of samples from cooling condition 1 but also in the steady-state region of samples from cooling condition 2, where a higher coating temperature was obtained. Horizontal delaminations are present between the lamellae, however, because the temperature of the underlying lamella is low compared to that of the first droplets forming the new lamella. It is worth noting that close to the bond coating of samples from cooling condition 1, the microstructure is the same as that of the other samples because the high steady-state temperature has not yet been reached.

4.2 *Density of Vertical Microcracks*

After solidification, the splats cool rapidly from melting point to the temperature of the underlying material, which at the same time slightly increases in temperature due to heat transport. The rapid cooling would be associated with a large shrinkage of the splat, but, assuming good mechanical contact between the splat and the underlying material, this contraction is hindered and large positive strains are created in the splat. Large tensile stresses are associated with these strains because the Young's modulus of zirconia is relatively high. These in-plane stresses are called "quenching stresses" and are always tensile independent of the material. Investigations on brittle ceramic materials such as alumina and zirconia show low quenching stresses (Ref 4), indicating that some relaxation must have occurred. The most important stress relaxation mechanism is believed to be the formation of vertical microcracks. When the tensile stresses in the splat reach the critical stress level, relaxation occurs through microcracking.

The extent of microcracks created in the splats thus depends on the temperature difference between the melting point and that of the underlying material. A large temperature difference means large strains, which cause large stress relaxation and a high density of vertical microcracks. Our results confirm this. A larger density of vertical microcracks was found close to the bond coating, where the temperature of the underlying material is rather low. Differences between the samples in the steady-state regions of the top coating can also be seen: Samples sprayed without cooling have a lower density of vertical microcracks compared to samples sprayed at high cooling (Table 3).

4.3 *Possible Effects of the Defects*

The existence of vertical microcracks in a brittle ceramic coating would seem to be detrimental. During service, however, they seem to be stable, and no propagation of the cracks is observed. From a mechanical point of view, they are associated with positive effects. They not only relax the buildup of tensile stresses during spraying but also increase the compliance of the coating. This is beneficial during service conditions; coatings with a high compliance will decrease the stress buildup due to the thermal expansion mismatch between the substrate and the coating.

The most important factor for a thermal barrier coating is thermal conductivity. A low thermal conductivity is reached when a high density of horizontal delaminations is present in the coating (Ref 5). The delaminations act as interfaces between solid ceramic layers, and the presence of such interfaces will obstruct heat transport. However, if the density of horizontal delaminations is too high, the cohesion of the coating will be insufficient. This is particularly important in the region close to the bond coating, where failure during service normally occurs by propagation of a horizontal delamination.

5. Conclusions

The temperature of the growing coating strongly influences the microstructure as well as the defect structure in ceramic overlay coatings. When the coating is sprayed at high coating temperatures, columnar grains of a relatively large grain size are formed. Few horizontal delaminations develop within the lamellae of the coating, and few vertical microcracks are found. When spraying occurs at low coating temperatures, the grains are still columnar but are considerably smaller. Horizontal delaminations occur both within and between the lamellae, and the density of vertical microcracks is considerably higher. Hence, the ceramic coating closer to the bond coating shows a high defect density regardless of cooling condition.

The low density of horizontal delaminations that results from spraying at a high substrate temperature is due to continued grain growth through the splats in a lamella. The contact zone between the splats is thus formed without introducing splat boundaries. When spraying is performed at a low substrate temperature, continued grain growth through the splats does not occur. Grains are thus nucleated in the newly arrived splat, leading to intersplat horizontal delamination and low cohesion between the splats.

The high density of vertical microcracks that results from spraying at low coating temperatures is caused by the high degree of stress relaxation when the splats cool from the melting point to the low temperature of the underlying material. The high delamination density is expected to reduce thermal conductivity, whereas the high vertical microcrack density is expected to increase coating compliance, thus relieving the stresses in the coating during subsequent service.

Acknowledgments

The authors wish to acknowledge the financial support of the Nordic Industrial Fund and the Swedish Research Council for Engineering Sciences. Special thanks are directed to Mr. Jan Wigren, Volvo Aero Corporation, for many valuable discussions and for providing the sample material.

References

1. R. McPherson, Review of Microstructure and Properties of Plasma Sprayed Ceramic Coatings, *Surf. Coat. Technol.*, Vol 39/40, 1989, p 173-181

2. L. Pawlowski and P. Fauchais, Thermal Transport Properties of Thermally Sprayed Coatings, *Int. Mater. Rev.*, Vol. 37(No. 6), 1992, p 271-289
3. P. Harmsworth and R. Stevens, Microstructure of Zirconia-Yttria Plasma-Sprayed Thermal Barrier Coatings, *J. Mater. Sci.*, Vol 27, 1992, p 616-624
4. S. Kuroda and T. Clyne, The Quenching Stress in Thermally Sprayed Coatings, *Thin Solid Films*, Vol 200, 1991, p 49-61
5. R. Taylor, J. Brandon, and P. Morrell, Microstructure, Composition and Property Relationships of Plasma-Sprayed Thermal Barrier Coatings, *Surf. Coat. Technol.*, Vol 50, 1992, p 141-149